Modeling Chloride Diffusion and Corrosion Initiation

Zine-Eddine KRIBES[1], Rachid CHERIF[1], Abdelkarim AÏT-MOKHTAR[1], Julia HOLZHAUER[2], Julien GANCE[2], Stéphanie BETELU[3]

[1] *LaSIE UMR CNRS 7356, La Rochelle Université, Avenue Michel Crépeau, 17042 La Rochelle Cedex 1, France.*

[2] *IRIS Instruments 1 Av. Buffon, 45100, Orléans France*

[3] *BRGM, 3 Av. Claude Guillemin, 45100, Orléans France*

ABSTRACT: The objective of this study is to develop a multi-species model for chloride diffusion in saturated cementitious materials, taking into account all ions present in the pore solution, as well as ion-ion and ion-solid interactions, including mineral dissolution and precipitation phenomena. The ionic flux is calculated using the Poisson–Nernst–Planck equation, which incorporates diffusion, ionic migration, and chemical activity mechanisms. The Langmuir model is employed to simulate the chemical binding of chlorides to the material (chloride isotherms). The initiation of steel reinforcement corrosion is also predicted based on the threshold chloride concentration at the steel–concrete interface.

The proposed model is applied to a reinforced mortar made with Portland cement, exposed to chlorides under laboratory conditions over a period of fifty years. To support the model in terms of input data, initial conditions, and boundary conditions, the chloride diffusion coefficient and porosity of the tested mortar were determined experimentally.

KEYWORDS: Durability, chloride diffusion, modelling, corrosion initiation, cementitious materials

I. INTRODUCTION

Reinforced concrete structures in marine environments experience deterioration over their service life due to the ingress of chloride ions. These ions, originating either from seawater or de-icing salts in cold regions, diffuse through the concrete cover and can trigger the corrosion of embedded steel reinforcement [1–3]. In saturated zones, where the concrete is fully submerged in seawater, chloride transport primarily occurs by natural diffusion under a concentration gradient [4,5].

This issue has been the subject of numerous experimental and numerical studies aimed at predicting chloride transport and corrosion initiation [6–9]. Various modeling approaches for reactive ion transport in porous cementitious materials have been proposed. Initially, single-species models based on Fick's law were developed [10]. These models consider only the concentration of chloride ions in the pore solution and neglect ionic interactions. Later, multi-species approaches were introduced, accounting for chemical and physical interactions during transport, such as chemical activity and the electrical double layer (EDL). In these models, ionic

flux is computed using the Nernst–Planck equation, which incorporates diffusion, migration, and chemical activity effects [11–16].

Corrosion initiation modeling relies on several approaches to predict the onset of corrosion at the steel–concrete interface [17–19]. Two main methods are commonly used: the first is based on the electric current intensity, a key parameter in electrochemical models that characterizes redox reaction kinetics and defines the critical chloride threshold for corrosion initiation. The second approach focuses on chloride diffusion, modeling the progressive ingress of aggressive agents until a critical concentration is reached at the steel surface, as defined by the NF EN 206 standard.

In this study, we propose a multi-species ionic transport and corrosion initiation model for saturated cementitious materials exposed to chlorides. The model considers all relevant ions in the pore solution, including ion–ion and ion–solid interactions, as well as mineral dissolution and precipitation processes. These chemical reactions are modeled through a thermodynamic approach based on the law of mass action [4,20-22]. The ions considered in the study include Cl^-, Na^+, K^+, OH^-, Ca^{2+}, and SO_4^{2-}. Ionic flux is computed using the Poisson–Nernst–Planck equation, which accounts for diffusion, migration, and chemical activity. Chloride binding is modeled using the Langmuir isotherm. This model is rarely used in the literature due to the mathematical complexity it entails.

Additionally, the corrosion current intensity is estimated through an empirical relationship based on the free chloride ion concentration near the reinforcement, located at a 5 cm cover depth. The model is applied to a reinforced mortar made with Portland cement and subjected to natural chloride diffusion under immersion. The initial composition of the pore solution is used as the starting condition. Furthermore, the chloride diffusion coefficient and water-accessible porosity of the mortar were experimentally measured to provide input data for the model. The outputs of the proposed model are:

(i) ionic concentration profiles for all considered species, and

(ii) the corrosion current intensity.

II. Modelling principle

II.1. Ionic reactive transport

Ionic transport is governed by the mass conservation equation (Eq. 1), which describes the time-dependent evolution of the concentration of ion i (C_i) during the transport process:

$$\varphi \frac{\partial C_i}{\partial t} + (1-\varphi)\frac{\partial C_{i,b}}{\partial t} = -\mathbf{div}(J_i) \pm q_i \qquad \text{(Eq. 1)}$$

where C_i [mol·m^{-3}] is the concentration of free ion i, $C_{i,b}$ [mol·m^{-3}] is the concentration of bound ions, J_i [mol·m^{-2}·s^{-1}] is the ionic flux, and q_i [mol·m^{-3}·s^{-1}] is the source term accounting for dissolution and precipitation phenomena during ionic transport.

In this study, the Langmuir model (Eq. 2) is used to calculate the chemical binding of chlorides as follows:

$$C_{Cl,b} = \frac{\alpha C_{Cl}}{1 + \beta C_{Cl}} \qquad \text{(Eq. 2)}$$

The ionic flux J_i is calculated using the Nernst–Planck equation (Eq. 3), which accounts for diffusion under a concentration gradient, migration and the chemical activity coefficient γ_i associated with ion–ion interactions.

$$J_i = -D_{ins,i}\left(\nabla C_i + \frac{z_i C_i F}{RT}\nabla\psi + C_i \nabla \ln\gamma_i\right) \quad \text{(Eq. 3)}$$

where $D_{ins,i}$ [m²·s⁻¹] is the diffusion coefficient of ion i, γ_i [–] is the activity coefficient of ion i, ψ [V] is the total electric potential, z_i [–] is the valence of ion i, and F [C·mol⁻¹] is the Faraday constant.

The electric potential ψ is computed using the Poisson equation, as given in Eq. (4) [23].

$$\Delta\psi + \frac{F}{\epsilon}\omega\left(\sum_{i=1}^{N} z_i C_i\right) = 0 \quad \text{(Eq. 4)}$$

where ε [C²·N⁻¹·m⁻²] is the electrical permittivity, and N [–] is the number of ionic species considered.

The ionic activity $\ln\gamma_i$ is calculated using the Davies model, as given in Eq. (5). This model is applicable to highly concentrated solutions, for ionic strengths I up to 1200 mol·m⁻³ [23].

$$\ln\gamma_i = \frac{-A_\gamma z_i^2\sqrt{I}}{1 + a_i B_\gamma\sqrt{I}} + \frac{C_\gamma A_\gamma z_i^2\sqrt{I}}{\sqrt{1000}} \quad \text{(Eq. 5)}$$

where $A\gamma$ [–] and $B\gamma$ [–] are the Debye–Hückel constants, and $C\gamma$ represents the Davies constant.

The source term (q_i) in Eq. (1), which reflects thermodynamic equilibrium, represents the involvement of ion i in the dissolution or precipitation of mineral m. The minerals considered in this study are Friedel's salt (Fds), Kuzel's salt (Kgs), monosulfoaluminates (AFm), and trisulfoaluminates (AFt).

The source term is calculated as the product of the stoichiometric coefficient ($n_{i,m}$) and the dissolution/precipitation rate of the mineral (r_m), as shown in Eqs. (6) and (7), in accordance with the work of Lasaga et al. [22] and Steefel et al. [24]. The rate of dissolution or precipitation depends on the evolution of ionic concentrations in the pore solution during chloride transport.

$$q_i = \sum n_{i,m} \times r_m \quad \text{(Eq. 6)}$$

$$r_m = \chi_m\left(1 - \frac{1}{K_m}\prod_{i=1}^{N_i}\{C_i\}^n\right) \quad \text{(Eq. 7)}$$

where χ_m [mol·m⁻²·s⁻¹] is the dissolution or precipitation rate constant of mineral m, and K_m [–] is the thermodynamic equilibrium constant of mineral m. The values of the dissolution/precipitation rate constants and the thermodynamic equilibrium constants are provided in Table 1.

TABLE 1. Kinetic constants (χ_m) and thermodynamic equilibrium constants (K_m) [21].

Minerals	χ_m [mol·m^{-2}·s^{-1}]	K_m
Fds	1E-5	1E-29.1
Kgs	1E-5	1E-73.2
AFm	6.8E-12	1E-29.3
AFt	7.1E-13	1E-44.0

It should be noticed that cementitious materials, due to their heterogeneous and reactive composition, consist of multiple mineral phases that continuously interact under thermodynamic equilibrium. These interactions lead to the formation of various hydration products, such as calcium silicate hydrates (C-S-H), portlandite, ettringite and monosulfoaluminates.

The diffusion of chloride ions through the cementitious matrix disturbs the chemical equilibrium between the solid phase and the pore solution [25]. This equilibrium is subsequently re-established through dissolution or precipitation reactions of solid phases, resulting in the formation of new minerals.

II.2. Corrosion Initiation

To predict the time required for corrosion initiation, we chose to monitor the corrosion rate through the current density associated with the chloride ion concentration near the reinforcement. For this purpose, the model proposed by Liu and Weyers [26], given in Equation (8), was used due to its ability to relate the chloride ion concentration to the corrosion current density (i_{corr}) near the steel surface.

Corrosion initiation is considered to occur when the corrosion current density reaches 0.1 µA/cm² [27], which allows for an estimation of the time needed for the onset of the corrosion process in reinforced concrete structures.

$$i_{corr} = \frac{1}{1,08} exp\left[8,37 + 0,618\, ln(1,69\, C_{Cl}) - \frac{3034}{T} - 0,105 \cdot 10^{-3} R_{be} + \frac{2,32}{t^{0,215}}\right] \quad \text{(Eq. 8)}$$

where T [K], R_{be} [Ω] and t [years] denote the temperature, the resistivity of the concrete cover, and time, respectively.

In this study, it was assumed that certain parameters remain constant within the mortar. The temperature T was fixed at 296 K, and similarly, the resistivity of the concrete cover R_{be} was maintained at 1200 Ω.

III. Case study

The proposed model is applied to a reinforced mortar immersed in a saline solution composed of deionized water and 500 mol/m³ of NaCl for a duration of fifty years. The objective is to simulate the ionic concentration profiles within the 5 cm-thick concrete cover at different exposure times. The mortar is based on CEM I 52.5 N cement and standardized sand, with a water-to-cement ratio of 0.6 and a sand-to-cement ratio of 3. The chemical composition of the cement used, along with the main clinker phases, is presented in Table 2.

TABLE 2. Chemical composition of the CEM I 52.5 N cement used and the main clinker phases.

Oxyd	CaO	SiO_2	Al_2O_3	Fe_2O_3	SO_3	K_2O	Na_2O	Chlorides
wt.%	64.20	20.50	5.00	3.90	2.5	0.29	0.05	1.4
Phases	C_3S		C_2S		C_3A		C_4AF	
wt.%	65		13		7		13	

To support the proposed modeling, an experimental investigation was conducted to measure the water porosity and the chloride ion diffusion coefficient of the tested mortar (input data for the model). The experimental procedure followed is described in the next section. However, the chemical composition of the mortar's pore solution (initial conditions for the model) and the chloride binding isotherms were taken from literature data on the same material [28].

III.1. Measurement of water porosity and chloride diffusion coefficient

The water porosity (φ) was measured according to the French standard NF P 18-459. The experimental protocol consists first of subjecting the tested material to vacuum suction using a desiccator to remove air bubbles, followed by immersion in water. After saturation, the saturated mass (*Ms*) and the mass of the sample in water (*Mw*, hydrostatic weighing) were determined. Subsequently, the samples were dried at 45 °C and weighed to obtain their dry mass (*Md*). Finally, the water porosity was calculated using Eq. (9):

$$\varphi = \frac{M_s - M_d}{M_s - M_w} \quad \text{(Eq. 9)}$$

The effective diffusion coefficient of chloride ions (DCl) was determined using a steady-state migration test. The migration cell consists of two compartments: the upstream compartment (2 l) contains a basic solution of 83 mol/m³ KOH, 25 mol/m³ NaOH, and 500 mol/m³ NaCl, while the downstream compartment (1 l) contains only the basic solution. Platinum electrodes are placed in each compartment (cathode upstream, anode downstream), and an electric field of 300 V/m is applied across the sample.

Tests were performed on cylindrical mortar discs (63 mm diameter, 10 mm thickness), pre-saturated under vacuum for 24 hours in the same basic solution. Chloride migration was monitored by titration in the downstream compartment using a 785 DMP Titrino titrator until steady state was reached. The diffusion coefficient D_{Cl} was then calculated using Eq. (10) [13].

$$D_{Cl} = \frac{RT}{z_{Cl^-}F}\frac{L}{E}\frac{\Delta C}{\Delta t}\frac{V_a}{A\,C_0}\left(1 - e^{\frac{z_{Cl^-}}{RT}FE}\right) \quad \text{(Eq. 10)}$$

where V_a [m³], ΔC [mol.m^{-3}], Δt [sec], A [m²], L [m], C_0 [mol.m^{-3}], U [V] and F [C.mol^{-1}], represent, respectively, the volume of the downstream compartment of the cell, the change in chloride ion concentration in the downstream compartment over the time interval Δt, the cross-sectional area and thickness of the sample, the chloride concentration in the upstream compartment, the potential difference applied across the sample and the Faraday constant.

The initial and boundary conditions applied in the simulations of immersion in saline solution under natural diffusion are summarized in Table 3. The results obtained facilitate the analysis of the chloride concentration profile and its temporal evolution near the reinforcement (with a 5 cm

concrete cover) in the tested material, enabling the evaluation of the time-dependent corrosion current of the reinforcement.

TABLE 3. Input data, initial conditions and boundary conditions used in the simulations.

Input data			
Parameter		Notation	Values
Porosity [%]		φ	25.1
Ion diffusion coefficients [x10^{-12} $m^2 \cdot s^{-1}$]		D_{Cl^-}	3.5
		D_{Na^+}	2.3
		D_{K^+}	3.4
		D_{OH^-}	8.1
		$D_{Ca^{+2}}$	2.7
		$D_{SO4^{-2}}$	3.7
Langmuir isotherm constants [-]		α	3.9 10^{-4}
		β	2.0 10^{-3}
Initial and boundary conditions			
	Upstream (x = 0, t) [mol·m^{-3}]	Downstream (x = L, t) [mol·m^{-3}]	(t = 0, 0 < x < L) [mol·m^{-3}]
C_{Cl^-}	500	500	4
C_{Na^+}	500	500	51
C_{K^+}	0	0	117
C_{OH^-}	0	0	164
$C_{Ca^{2+}}$	0	0	2
$C_{SO4^{2-}}$	0	0	2

It should be noticed that in the prepared solution, the contribution of ions resulting from the auto-ionization of water (H^+ and OH^-) is negligible. Indeed, their concentration (< 10^{-3} mol·m^{-3}) is significantly lower than that of the predominant ions, such as Cl^- and Na^+ (500 mol·m^{-3})[3]).

IV. Results and discussion

Fig. 1 shows the simulated chloride profiles in the tested mortar after 0.5, 1, 2, 4, and 50 years of exposure to the saline solution. The concentration of free Cl^- ions gradually increases within the material due to diffusion from the external solution driven by the concentration gradient. Near the reinforcement, this concentration evolves over time: between 0.5 and 1 year, it increases by 0.4%, then by 5.8% between 1 and 2 years, indicating an acceleration of the diffusion process. In contrast, between 2 and 4 years, the growth rate slows to 3.6%. After 4 years of exposure, the chloride concentration near the reinforcement reaches 129 mol·m^{-3}. By 50 years, the concentration has reached its maximum.

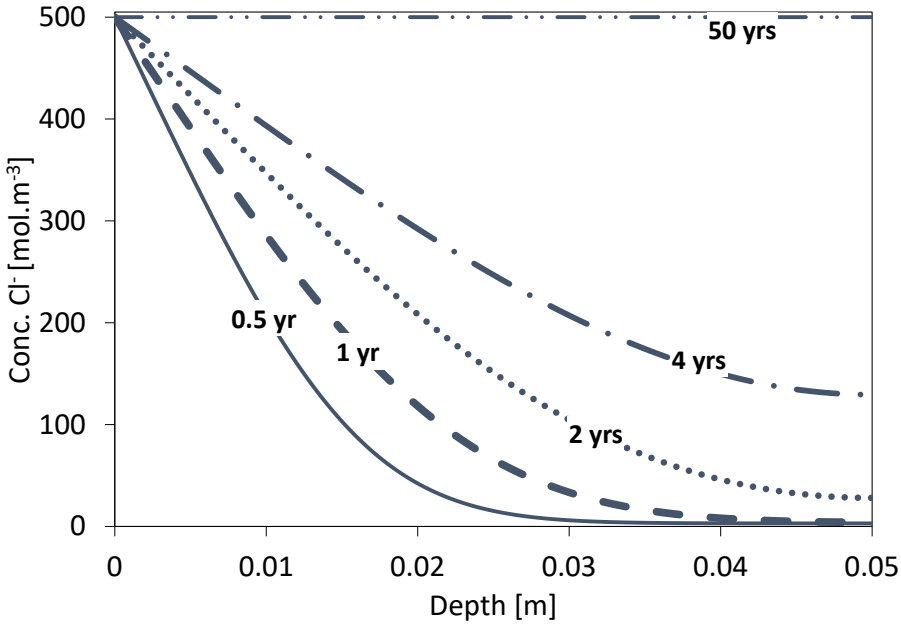

FIGURE 1. Simulated chloride ion concentration profiles in the tested mortar after 0.5, 1, 2, 4, and 50 years of immersion in a saline solution.

Fig. 2 illustrates the evolution of the corrosion current density of the reinforcement over a 50-year immersion period, calculated using Eq. (8) based on the simulated chloride concentration near the reinforcement. A gradual increase in current density is observed over time. According to the literature, a current density of 0.1 μA·cm^{-2} [27] is considered the threshold for corrosion initiation. Based on this criterion, the time to corrosion initiation is estimated at 2.4 years (see Fig. 2), corresponding to a chloride concentration of 34 mol·m^{-3}.

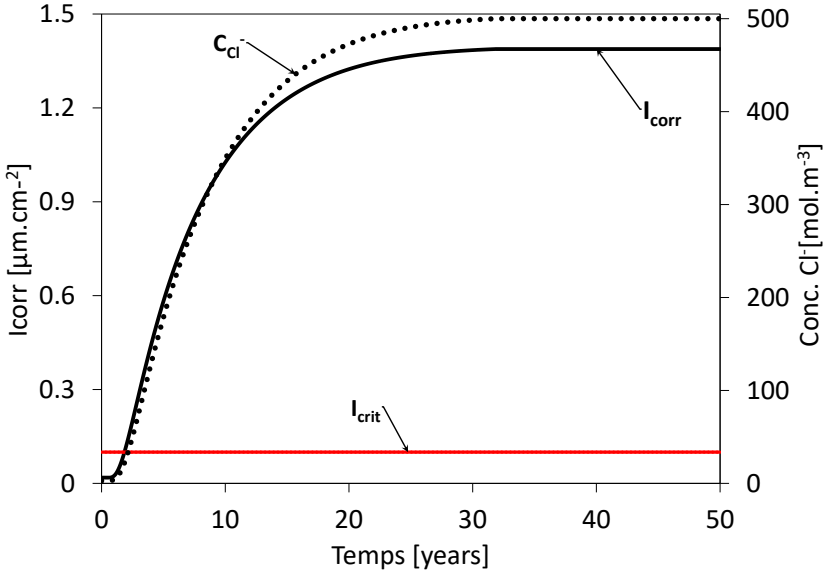

FIGURE 2. Evolution of reinforcement corrosion current density and chloride ion concentration over 50 years of immersion in a saline solution.

V. Conclusion

The following conclusions can be drawn from the results obtained:

- The proposed model successfully simulates ion transport in saturated cementitious materials, accounting for both the pore solution composition and dissolution–precipitation phenomena. Although applied here to mortar, the model is general and can be adapted to other types of cement-based materials (e.g., Portland cement concrete with mineral additions).
- The results include the evolution of chloride ion concentration profiles within the exposed material. These profiles were used to calculate the corrosion current of the reinforcement, thereby assessing the corrosion state of the steel.
- Finally, future work could extend the model to unsaturated environments (e.g., tidal zones) and incorporate additional dissolution/precipitation mechanisms, particularly those related to C-S-H phases.

ACKNOWLEDGEMENT

The authors would like to thank the project ANR El-TORO CE42-AAPG 2021 (French agency of research) for funding this work.

REFERENCES

[1] C. Li, X. Song, L. Jiang, A time-dependent chloride diffusion model for predicting initial corrosion time of reinforced concrete with slag addition, Cem. Concr. Res. 145 (2021) 106455. https://doi.org/10.1016/j.cemconres.2021.106455

[2] Q. Li, W. Zhang, W. Shao, D. Shi, Numerical modeling of non-uniform corrosion of concrete reinforcement considering calcium leaching and chloride diffusion coupling effect, Corros. Sci. 237 (2024) 112343. https://doi.org/10.1016/j.corsci.2024.112343

[3] O. Poupard, A. Aït-Mokhtar, P. Dumargue, Impedance spectroscopy in reinforced concrete: Experimental procedure for monitoring steel corrosion. Part II Polarization effect, J. Mater. Sci. 38 (2003) 3521-3526. DOI: 10.1023/A:1025600624991

[4] Z.-E. Kribes, R. Cherif, A. Aït-Mokhtar, Modelling of Chloride Transport in the Standard Migration Test including Electrode Processes, Materials 16 (2023) 6200. https://doi.org/10.3390/ma16186200

[5] HE. Álava, E. Tsangouri, N. De Belie, G. De Schutter, Chloride interaction with concretes subjected to a permanent splitting tensile stress level of 65%, Constr. Build. Mater. 127 (2016) 527–538.

[6] C. Andrade, Calculation of chloride diffusion coefficients in concrete from ionic migration measurements, Cement and Concrete Research 23 (1993) 724–742. https://doi.org/10.1016/0008-8846(93)90023-3

[7] O. Truc, JP. Ollivier, M. Carcassès, A new way for determining the chloride diffusion coefficient in concrete from steady state migration test, Cem. Concr. Res. 30 (2000) 217-226.

[8] H. Friedmann, O. Amiri, A. Aït-Mokhtar, P. Dumargue, A direct method for determining chloride diffusion coefficient by using migration test, Cem. Concr. Res. 34 (2004) 1967-1973.

[9] S. Chen, H. Zhuang, Y. Zhou, S. Li, C. Li, Numerical simulation of chloride-induced reinforcement corrosion in cracked concrete based on mesoscopic model, Construction and Building Materials 441 (2024) 137408. https://doi.org/10.1016/j.conbuildmat.2024.137408

[10] S. Chatterji, On the applicability of Fick's second law to chloride ion migration through portland cement concrete, Cem. Concr. Res. 25 (1995) 299–303. https://doi.org/10.1016/0008-8846(95)00013-5

[11] O. Amiri, A. Aït-Mokhtar, A. Seigneurin, A complement to the discussion of A. Xu and S. Chandra about the paper "Calculation of chloride coefficient diffusion in concrete from ionic migration measurements" by C. Andrade, (1997). https://doi.org/10.1016/S0008-8846(97)00082-3

[12] L.Y. Li, C.L. Page, Modelling of electrochemical chloride extraction from concrete: Influence of ionic activity coefficients, Computational Materials Science 9 (1998) 303–308. https://doi.org/10.1016/S0927-0256(97)00152-3

[13] O. Amiri, A. Aït-Mokhtar, P. Dumargue, G. Touchard, Electrochemical modelling of chlorides migration in cement based materials. Part II: Experimental study—calculation of chlorides flux, Electrochimica Acta 46 (2001) 3589–3597. https://doi.org/10.1016/S0013-4686(01)00659-4

[14] O. Amiri, H. Friedmann, A. Aït-Mokhtar, Modelling of chloride-binding isotherm by multi-species approach in cement mortars submitted to migration test, Magazine of Concrete Research 58 (2006) 93–99. https://doi.org/10.1680/macr.2006.58.2.93

[15] X. Yu, J. Li, Y. Yu, A. Song, Advancing service life estimation of reinforced concrete considering the coupling effects of multiple factors: Hybridized physical testing and machine learning approach, J. Build. Eng. 84 (2024) 108476. https://doi.org/10.1016/j.jobe.2024.108476

[16] J.-C. Park, H.-J. Jung, Finite element method-based numerical study utilizing experimental data on chloride solution transport in concrete under hydraulic pressure, Constr. Build. Mater. 418 (2024) 135270. https://doi.org/10.1016/j.conbuildmat.2024.135270

[17] M. Ohno, P. Limtong, T. Ishida, Multiscale modeling of steel corrosion in concrete based on micropore connectivity, Journal of Building Engineering 47 (2022) 103855. https://doi.org/10.1016/j.jobe.2021.103855

[18] H. Wang, W. Zhu, S. Qin, Y. Tan, Numerical simulation of steel corrosion in chloride environment based on random aggregate concrete microstructure model, Construction and Building Materials 331 (2022) 127323. https://doi.org/10.1016/j.conbuildmat.2022.127323

[19] L. Dudi, S. Krishnan, S. Bishnoi, Numerical modeling for predicting service life of reinforced concrete structures exposed to chloride, Journal of Building Engineering 79 (2023) 107867. https://doi.org/10.1016/j.jobe.2023.107867

[20] B. Guo, Y. Hong, G. Qiao, J. Ou, Z. Li, Thermodynamic modeling of the essential physicochemical interactions between the pore solution and the cement hydrates in chloride-contaminated cement-based materials, Journal of Colloid and Interface Science 531 (2018) 56–63. https://doi.org/10.1016/j.jcis.2018.07.005

[21] R. Cherif, A.E.A. Hamami, A. Aït-Mokhtar, W. Bosschaerts, Thermodynamic equilibria-based modelling of reactive chloride transport in blended cementitious materials, Cement and Concrete Research 156 (2022) 106770. https://doi.org/10.1016/j.cemconres.2022.106770

[22] A.C. Lasaga, J.M. Soler, J. Ganor, T.E. Burch, K.L. Nagy, Chemical weathering rate laws and global geochemical cycles, Geochimica et Cosmochimica Acta 58 (1994) 2361–2386. https://doi.org/10.1016/0016-7037(94)90016-7

[23] E. Samson, J. Marchand, Numerical Solution of the Extended Nernst–Planck Model, Journal of Colloid and Interface Science 215 (1999) 1–8. https://doi.org/10.1006/jcis.1999.6145

[24] C.I. Steefel, C.A.J. Appelo, B. Arora, D. Jacques, T. Kalbacher, O. Kolditz, V. Lagneau, P.C. Lichtner, K.U. Mayer, J.C.L. Meeussen, S. Molins, D. Moulton, H. Shao, J. Šimůnek, N. Spycher, S.B. Yabusaki, G.T. Yeh, Reactive transport codes for subsurface environmental simulation, Comput Geosci 19 (2015) 445–478. https://doi.org/10.1007/s10596-014-9443-x

[25] L. Sutter, K. Peterson, S. Touton, T. Van Dam, D. Johnston, Petrographic evidence of calcium oxychloride formation in mortars exposed to magnesium chloride solution, Cement and Concrete Research 36 (2006) 1533–1541. https://doi.org/10.1016/j.cemconres.2006.05.022

[26] Y. Liu, R.E. Weyers, Modeling the Time-to-Corrosion Cracking in Chloride Contaminated Reinforced Concrete Structures, MJ 95 (1998) 675–680. https://doi.org/10.14359/410

[27] D.A. Koleva, N. Boshkov, K. Van Breugel, J.H.W. De Wit, Steel corrosion resistance in model solutions, containing waste materials, Electrochimica Acta 58 (2011) 628–646. https://doi.org/10.1016/j.electacta.2011.10.010

[28] S. Pradelle, M. Thiery, V. Baroghel Bouny, Comparison of existing chloride ingress models within concretes exposed to seawater, Materials and Structures 49 (2016) 4497–4516. https://doi.org/10.1617/s11527-016-0803-y